ELSEVIER

Biochimica et Biophysica Acta 1329 (1997) 74–84

BIOCHIMICA ET BIOPHYSICA ACTA
BBA

Estimating the electrostatic potential at the acetylcholine receptor agonist site using power saturation EPR

George H. Addona [1], Scott H. Andrews, David S. Cafiso *

Department of Chemistry and Biophysics Program at the University of Virginia, Charlottesville, VA 22901, USA

Received 2 December 1996; revised 24 March 1997; accepted 3 April 1997

Abstract

Continuous wave EPR power saturation was used to measure electrostatic potentials at spin-labeled sites. Membrane surface potentials were estimated by power saturating the EPR spectrum of a membrane bound ^{14}N spin-labeled amphiphile in the presence of a neutral or positively charged ^{15}N labeled aqueous spin probe. The potentials that are measured are in good agreement with other probe measurements and with the predictions of the Gouy–Chapman–Stern theory, indicating that this is a valid approach to determine electrostatic potentials. A spin-labeled affinity probe based on maleimidobenzyltrimethylammonium was synthesized and could be derivatized to a sulfhydryl near either agonist site on the nicotinic acetylcholine receptor. The amplitudes of motion of the spin-probe on the ns time scale are significantly different when the two labeled sites are compared, and the probe is more restricted in its motion when attached to the more easily labeled site. When attached to this agonist site, power saturation EPR yields an electrostatic potential of −15 mV. Two other sulfhydryl-specific probes were used to label this site in reconstituted receptor containing membranes. These probes show less contact with the receptor and reduced electrostatic potentials, indicating that there is a strong spatial dependence to the potential at the agonist site. This work demonstrates that power saturation EPR provides a general method that can be used to estimate electrostatic potentials at any specifically spin-labeled macromolecular site. © 1997 Elsevier Science B.V.

Keywords: Spin labeling; Ligand gated ion channel; Electrostatics; Surface potential; Sulfhydryl probe

1. Introduction

The nicotinic acetylcholine receptor (AChR) is a ligand-gated ion channel located at the postsynaptic membrane of the neuromuscular junction. It is composed of five subunits with a stoichiometry of $\alpha_2\beta\delta\gamma$ [1], with two agonist binding sites one on each α-subunit. The two agonist binding sites are not equivalent and there is evidence from covalent labeling and from cross-linking studies that the acetylcholine binding sites are located at the α–γ and α–δ subunit interfaces [2,3]. Several studies using affinity labeling have provided evidence that Tyr^{93}, Trp^{149}, Tyr^{190}, Cys^{192}, Cys^{193} and Tyr^{198} from the α-subunit participate in the agonist site [4–6].

It has been known for some time that there is a readily reducible disulfide bond within 10 Å of the acetylcholine binding site that is formed by Cys^{192} and Cys^{193} [7,8]. By reducing the receptor with dithiothreitol (DTT), the cholinomimetic affinity reagent 4-(*N*-maleimido)benzyltri[^{3}H]methyl ammo-

* Corresponding author. Fax: (+1) (804) 924-3710.
[1] Present address: Department of Anesthesiology, Massachusetts General Hospital, Boston, MA 02114-2636, USA.

PII S0005-2736(97)00089-8

nium (MBTA) can be incorporated into one of the acetylcholine binding sites [9]. The only other disulfide bonds in the α-subunit are Cys^{128}–Cys^{142} and Cys^{412}–Cys^{418} and they have been shown to be completely resistant to mild reduction, requiring $NaBH_4$ to reduce the disulfide bond [10]. The second site can be derivatized if labeling is carried out in the presence of DTT [11]. Through the use of a cross-linking reagent, aspartate or glutamate residues that are located within 10 Å of a Cys^{192}/Cys^{193} have been identified. These include residues located in the δ-subunit between positions 164–224 [3]. Removal of these negative residues, particularly Asp^{180} and Glu^{189}, by site-directed mutagenesis was found to significantly weaken the affinity of the agonist site for acetylcholine [12]. Recently, electrostatic potentials were estimated at this site by examining the kinetic salt effect for charged thiosulfonates [13]. The potentials estimated using this technique were negative by about 30 mV, consistent with the presence of acidic residues at the agonist site.

Electrostatic potentials on proteins and membrane surfaces play crucial roles in the molecular function of biological systems [14,15], and both computational and experimental approaches can be taken to investigate their magnitude. One very powerful approach to estimate macromolecular potentials involves the use of spin-labeling and electron double resonance (ELDOR). In this approach, electrostatic potentials at a site can be determined by measuring the collisional frequency between charged or uncharged water-soluble nitroxides and a nitroxide attached to the macromolecule [16]. ELDOR provides a measure of the Heisenberg spin exchange rate, which reflects the frequency of collisions between paramagnetic species [17,18]. This is used to provide a direct measure of the concentration of the soluble nitroxide. This approach has a number of advantages over methods that utilize probe partitioning and it does not suffer from some difficulties that can be encountered in fluorescence measurements. However, this approach requires EPR equipment that is not widely available.

In the present study, we describe the synthesis and characterization of a spin-label (**I**) based on the affinity reagent MBTA shown below. We show that this label can be attached to one or both agonist sites on the AChR, and we use this label to investigate the accessibility, and the dynamics of the spin-label at the two agonist sites. We also demonstrate that continuous wave power saturation EPR spectroscopy can be used to measure collisional exchange between ^{15}N and ^{14}N nitroxide spin labels, and we use this approach to estimate the electrostatic potential at the agonist site labeled by probes **I**, **II**, **III** and on membrane surfaces labeled by the paramagnetic amphiphile **IV**.

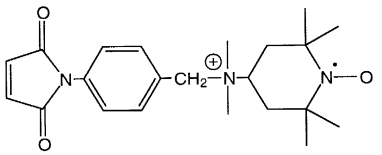

I

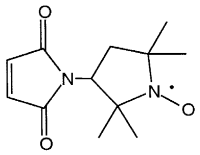

II

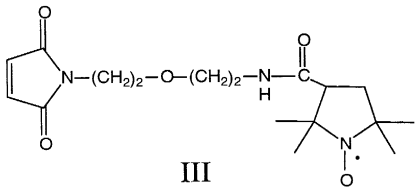

III

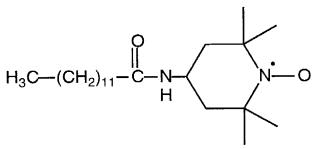

IV

2. Materials and methods

2.1. Materials

Egg phosphatidylcholine (egg PC) and phosphatidylserine were obtained from Avanti Polar Lipids (Birmingham, AL). Bromoacetylcholine bromide was synthesized following a procedure described elsewhere [19]. Acrylamide, bis-acrylamide, sodium dodecylsulfate (SDS), and Affigel-10 were obtained from BioRad Laboratories (Richmond, CA). Mercaptoethanol, cystamine hydrochloride, iodoacetamide, phenylmethylsulfonylfluoride (PMSF), carbamylcholine, cholic acid, dithiothreitol (DTT), glycine, tricine and Trizma were from Sigma (St. Louis, MO). The cholic acid was recrystallized five times from 95% ethanol before use. MOPS was obtained from Calbiochem (San Diego, CA). Nickel(II) ethylenediaminediacetic acid (NiEDDA) and *N*-tempoyl dodecylamide (**IV**) were gifts of Dr. Wayne Hubbell. Nickel acetylacetonate hydrate (NiAA) and potassium chromium oxalate trihydrate (CROX), maleic anhydride, *N*-bromosuccinimide (NBS), *p*-toluidine, benzoyl peroxide, maleimido-proxyl (**II**), maleimidoethoxyethylcarbamoyl proxyl (**III**), and aminotempo were obtained from Aldrich Chemical Co. (Milwaukee, WI). *p*-Toluidine was recrystallized from 95% ethanol and NBS was recrystallized from water after filtering solid contaminates. The isotopically labeled nitroxides, ^{15}N amino-tempo (**VI**) and ^{15}N hydroxy-tempo (**V**) were obtained from MSD Isotopes (Montreal, Canada). Liquid nitrogen frozen electroplax from *Torpedo californica* and *Torpedo nobiliana* were obtained from Pacific Biomarine, Venice CA and Biofish Associates, Boston MA, respectively.

2.2. Preparation of phospholipid vesicles

To prepare lipid samples of varying surface potential, chloroform stock solutions of egg PC and PS were mixed in the appropriate proportion, rotoevaporated and dried overnight in a vacuum desiccator. For each sample, an appropriate amount of 100 mM KCl, 1 mM MOPS buffer of pH 7.0 was added to the dried lipid to give a final concentration of approximately 50 mg/ml lipid. The lipid was vortexed and the resulting lipid solution freeze–thawed 6 times. Unilamellar vesicles were formed by passing the lipid solution through 0.05-μm pore size polycarbonate membrane filters (Poretics Corp, Livermore, CA) using a Lipofast syringe extruder (Avestine, Canada). Nineteen passes were made through the filters. Vesicles were stored under argon and refrigerated until used. Lipid concentrations were determined using a modified Fiske–Subbarrow procedure [20]. The *N*-tempoyl dodecylamide spin label was added directly to the vesicle suspension at a concentration of approximately 50 μM.

2.3. Preparation of reconstituted AChR membranes

Receptor-rich membranes and reconstituted AChR (rAChR) samples were prepared from liquid N_2 frozen electroplax tissue from *T. californica* or *T. nobiliana* using a procedure described previously [21,22] in a lipid mixture consisting of DOPC/DOPA/cholesterol, 63:12:25. The total protein content of both native and reconstituted membranes was determined as described [23], and lipid concentrations were obtained by phosphate assay using a modified Fiske–Subbarrow procedure [20]. The typical lipid : protein ratios used in this sample were 400:1. Gel electrophoresis was performed using the discontinuous method [24], and the rAChR displayed the four bands corresponding to the four receptor subunits with a purity that was greater than 95% as judged by the stain density.

2.4. Synthesis of the MBTA spin label, *I*

A solution of maleic anhydride (1.2 eq) in chloroform was added slowly to a stirred solution of recrystallized, dry *p*-toluidine in chloroform. After 1 h, the resulting *N*-(4-α-methylphenyl) maleamic acid crystals were collected and excess maleic anhydride removed by rinsing the crystals with chloroform. Three grams of *N*-(4-α-methylphenyl) maleamic acid was dissolved in approximately 6 ml of acetic anhydride containing 500 mg sodium acetate. Cyclization to 4-(*N*′-maleimido)-toluene was completed by heating for 30 min. The mixture was poured into ice water, extracted twice with chloroform and the organic layer dried by rotory evaporation. Mass spectrometry yielded the appropriate molecular weight of $m/z =$ 187. This product was converted to 4-(*N*′-maleimido)-benzylbromide by refluxing 1.5 g in 30 ml of benzene containing 2.0 g of NBS and 200 mg

benzoyl peroxide for 8 h. The product, 4-(*N*′-maleimido)-benzylbromide, was recrystallized in 95% ethanol and yield an $m/z = 266$ by mass spectrometry.

Dimethylamino-tempo was produced by refluxing 1 g of amino-tempo in methanol with the addition of 11 equivalents of 35% formaldehyde for 1 h. To the mixture, 3.5 equivalents of sodium borohydride was added and the reaction was allowed to proceed overnight at room temperature. Water was added to the mixture and extracted with chloroform. The organic layer was dried with sodium sulfate and removed under reduced pressure. The dimethylamino-tempo yielded an m/z of 199. The MBTA analog was synthesized by reacting 1.2 equivalents of 4-(*N*′-maleimido)-benzylbromide with *N*- dimethylamino-tempo in dry THF for 24 h. The salt precipitate was collected and washed with THF. The MBTA analog was purified by reverse-phase HPLC on a C18 column using a gradient of 0–80% water/acetonitrile. Fractions were screened by EPR for detection of a nitroxide. The spin label compound eluted at 38% acetonitrile. The identity of the spin label product was confirmed by mass spectrometry which yielded an $m/z = 385$. The sulfhydryl reactivity of the label was tested by reacting it with a cysteine containing peptide, ALCTWFPVL. The spin-labeled product gave an EPR spectrum that was characteristic of a nitroxide labeled peptide and the product had the anticipated value of $m/z = 1435$ as determined by mass spectrometry.

2.5. Labeling of reconstituted AChR with maleimide labels

Typically, 1.3 mg of rAChR in buffer A (100 mM NaCl, 10 mM MOPS, 0.1 mM EDTA, 0.02% sodium azide) was treated with 20 mM NEM overnight at 4°C, in order to block any free sulfhydryls. Excess NEM was removed by pelleting and resuspending rAChR vesicles 3 times in a Beckman Airfuge. The rAChR was then mildly reduced with 500 μM DTT for 1 h at room temperature. The unreacted DTT was removed by 3 centrifugation cycles. Spin labels **I**, **II** or **III** were added to a concentration of 100 μM to the reduced receptor and allowed to react for 1 h at room temperature. Free spin label was removed by 3 centrifugation cycles. The washed pellet was typically resuspended in 10 μl buffer A.

2.6. EPR spectroscopy

EPR measurements were performed using a Varian E-Line Century Series EPR spectrometer equipped with an X-band loop-gap resonator. Spectra were recorded from samples in quartz capillary tubes using a microwave power of 2 mW and a peak-to-peak modulation amplitude of 1.6 G. Gas permeable TPX capillaries were used for the power saturation experiments. Power saturation curves were obtained by measuring the peak-to-peak amplitude of the first derivative $m_1 = 0$ EPR line as a function of the microwave power in the range of 0.05–70 mW and plotted against the square root of the microwave power. The power saturation curves were fitted to the function:

$$A_{m_1=0} = IP^{1/2}\left[1 + (2^{1/\epsilon} - 1)\frac{P}{P_{1/2}}\right]^{-\epsilon} \quad (1)$$

where A is a constant, $P_{1/2}$ is the microwave power where the first derivative amplitude is reduced to half its unsaturated value and ϵ is measure of homogeneity of the saturation which varies from 0.5 to 1.5 [25]. As described below, values of $P_{1/2}$ were used to estimate changes in T_{1e}, the electron spin-lattice relaxation time in the presence of other paramagnetic species.

The paramagnetic metal complex NiEDDA was used at a concentration of 10 mM unless otherwise noted. For measurements on lipid bilayers, the uncharged and charged aqueous ^{15}N spin labels, **V** and **VI** shown below, were used at a concentration of 2 mM. In experiments involving the rAChR, the ^{15}N spin labels were used at a concentration of 1 mM. The depth of the alkyl amine nitroxide **IV** in lipid bilayers was estimated as described previously by measuring the effects of oxygen and the paramagnetic metal complex, NiEDDA on the power saturation behavior of the nitroxide [25].

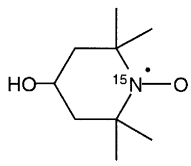

V

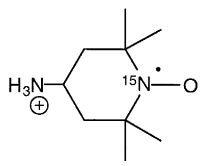

VI

2.7. Theory

Heisenberg exchange is a process that occurs when nitroxides undergo collisions resulting in an exchange of magnetization between interacting spin pairs. This is a short-range interaction where the collision radius is on the order of 4 Å for the six membered nitroxides used here [18]. Dipole–dipole interactions can also take place between nitroxides; however, in non-viscous media, such as aqueous solutions, Heisenberg exchange is the dominant process [17]. Heisenberg or spin-exchange with an ^{15}N nitroxide species will provide an additional relaxation pathway for ^{14}N nitroxides and will enhance the spin-lattice relaxation rate, R_{1e}, of the electron. Following an approach that utilized ELDOR spectroscopy [16], the $P_{1/2}$ value for one of the ^{14}N spin labels **I–III**, shown above, was measured in the presence and absence of one of the two ^{15}N labels **V** or **VI**. These $P_{1/2}$ values were used to provide an estimate of the local concentration of the charged and uncharged nitroxide at the ^{14}N labeled site.

The $P_{1/2}$ value is proportional to the product of R_1, the electron spin-lattice relaxation rate, and R_2, the electron spin-spin relaxation rate. In the case where the electron is being relaxed by a metal ion with a rapid relaxation rate, the value of $\Delta P_{1/2}$ can be directly related to W_{ex}, or the Heisenberg exchange frequency as shown in Eq. (2) [26].

$$\Delta P_{1/2} \propto P_{1/2} - P^0_{1/2} = R_2 R_1 - R^0_2 R^0_1 \approx R^0_2 2W_{ex} \quad (2)$$

Here $P_{1/2}$ and $P^0_{1/2}$ represent the $P_{1/2}$ values in the presence and absence of the paramagnetic species, respectively, and R^0_1 and R^0_2 represent the spin-lattice and spin-spin relaxation rates in the absence of the ^{15}N nitroxide. In the present case, the relaxation rate of the ^{14}N nitroxide is expected to be enhanced by the presence of the ^{15}N label, and the above approximation should be appropriate as long as the exchange rates are small. Because R_1 is expected to be much more sensitive to collisions than R_2 [18], the assumption will be made that changes in $P_{1/2}$ in the presence of ^{15}N labels are directly proportional to the Heisenberg exchange frequency and hence the rate of collisions between ^{14}N and ^{15}N nitroxide labels.

The potential at a site on a macromolecular surface at a position r, ψ_r, will be related to the concentration of a charged species in the bulk phase, C_o, and the concentration at that site C_r. Solution non-idealities will be ignored, which is justified if the ionic environments are relatively similar between r and in the bulk phase. In this case,

$$\Psi_r = -\frac{zF}{RT}\ln\frac{C_r}{C_o} \quad (3)$$

where z, F and R have the usual meanings. The Heisenberg exchange rate, W_{ex}, between a bound ^{14}N nitroxide and ^{15}N nitroxide species in solution will be proportional to the concentration of ^{15}N spins. Since the exchange rate W_{ex} is expected to be roughly proportional to R_{1e} for the ^{14}N nitroxide system, the concentration of ^{15}N label at the ^{14}N nitroxide site will then be proportional to the values of $\Delta P_{1/2}$, and we can write:

$$\Psi_r = -\frac{zF}{RT}\ln\frac{\Delta P^z_{1/2}}{\Delta P^0_{1/2}} \quad (4)$$

where $\Delta P^0_{1/2}$ is the value of $\Delta P_{1/2}$ obtained in the presence of an uncharged aqueous ^{15}N label and $\Delta P^z_{1/2}$ is the value of $\Delta P_{1/2}$ obtained in the presence of a charged aqueous ^{15}N label of valence z.

3. Results

3.1. Covalent derivatization of the AChR with MBTA-SL

Shown in Fig. 1A is an EPR spectrum obtained from a sample of rAChR that was treated with NEM followed by mild reduction with DTT and labeling with probe **I**. Fig. 1B shows the EPR spectrum of an identical rAChR sample recorded under the same conditions, except that the mild DTT reduction was omitted. Relatively little nitroxide is incorporated into the sample without mild DTT treatment, and NEM treatment was very effective at blocking any reactive sulfhydryls. This procedure is believed reduce Cys^{192}/Cys^{193} and allow access of sulfhydryl reactive reagents into this site [9]. The ratio of spin labels per protein was estimated from the sample protein concentration by comparing the double integral of the spectrum shown in Fig. 1A with that for a series of standard concentrations of **I**. The nitroxide to protein ratio was approximately one spin label per protein

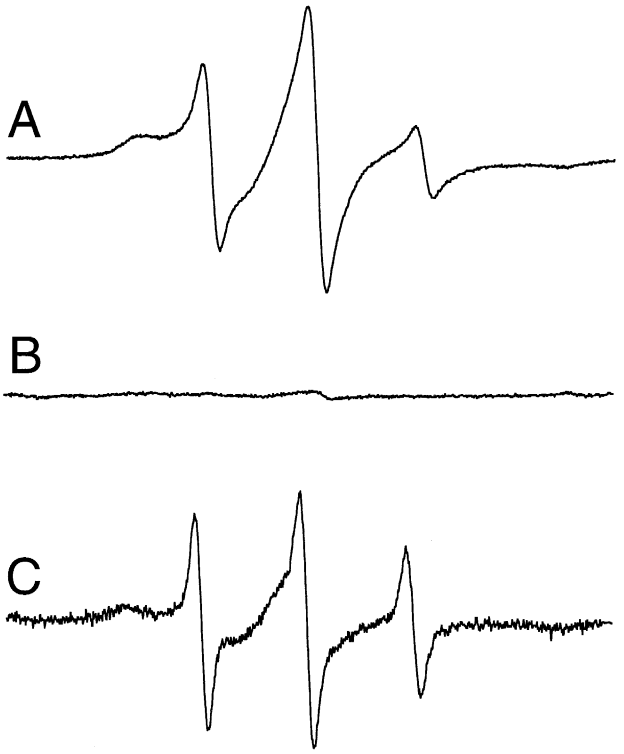

Fig. 1. EPR spectra of rAChR derivatized with the MBTA spin label. A: labeling of the rAChR following NEM labeling and DTT treatment. B: no DTT treatment. C: labeling in the presence of DTT.

consistent with the extent of labeling found for MBTA under similar conditions. Thus, apparently only one of the two acetylcholine binding sites was spin labeled under these conditions. We did not attempt to localize the label by sequencing, but previous sequencing data on MBTA indicates that it is predominantly Cys^{192} that is labeled [9]. It is known that labeling of both α-subunits can be achieved if the alkylation is done in the presence of DTT [11]. To label both sites with **I**, the same procedure used for the spectrum in Fig. 1A was followed, except that the label was added to a final concentration of 600 μM in the presence of DTT. The spectrum obtained after extensive washing of the sample by centrifugation is shown in Fig. 1C. The EPR spectrum shown in Fig. 1C represents a composite of both the high and low affinity AChR sites. As is readily apparent by comparison with Fig. 1A, motion of the nitroxide on the ns time scale is substantially greater at this second site. The sample used to obtain the EPR spectrum in

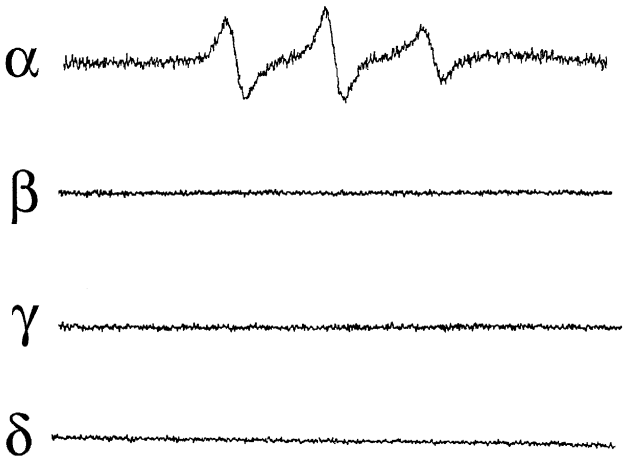

Fig. 2. EPR spectra of the AChR subunits extracted from SDS gel slices. Spectra were recorded at comparable spectrometer settings and provide a relative indication of the levels of spin-labeling in each subunit.

Fig. 1C was extensively washed until no further change in the EPR signal was detected, and no free spin could be detected in the supernatant.

If probe **I** is selectively incorporated into either Cys^{192} or Cys^{193} only the α-subunit should be labeled. To test this prediction, reconstituted AChR was labeled with **I** following the protocol used in Fig.

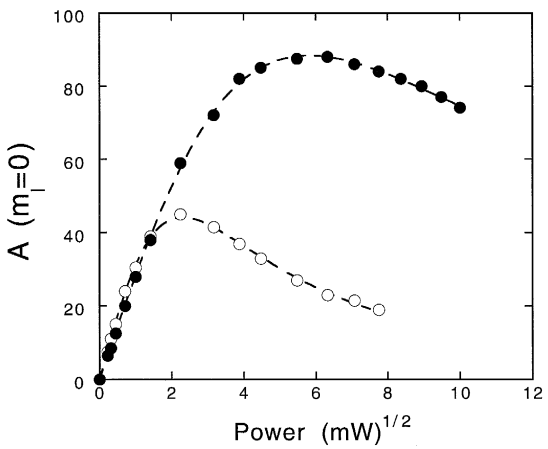

Fig. 3. Power saturation EPR spectra of the MBTA spin-label analog I, derivatized to the agonist site on the AChR, in the presence (●) and absence (○) of O_2. The dashed lines represent fits to the data using Eq. (1), and yielded values of $P_{1/2}$ of 6.0 and 37.0 mW in the presence of N_2 or 100% O_2, respectively. Power saturation of DPPH samples yielded values of $P_{1/2}$ of approximately 31 mW.

1A. The protein subunits were resolved by SDS–PAGE and the EPR spectra for the subunits excised from the gel were recorded. As seen in Fig. 2, the only the α-subunit had a measurable level of nitroxide incorporation. Since the only disulfide that becomes reduced in the α-subunit under the conditions used here is the disulfide between Cys^{192} and Cys^{193}, the label must reside at one of these positions.

Additional information about the nature of the site to which the nitroxide is associated can be obtained using power saturation experiments. Shown in Fig. 3 is a power saturation curve for **I** in the presence and absence of O_2. The $\Delta P_{1/2}$ value obtained from these data is 30.9 mW. When calibrated against a standard sample of DPPH (2,2-diphenyl-1-picryl-hydrazyl), which gave a $P_{1/2}$ of 31 mW, this accessibility was intermediate between values obtained for exposed nitroxides buried in the hydrocarbon core of membranes and nitroxides that face the aqueous phase [27].

3.2. Covalent derivatization of the AChR with other maleimides

In addition to probe **I**, spectra were also compared for the purified AChR labeled with the maleimido proxyl nitroxides, **II**, and the longer chain probe **III**. Even though these probes are not specific for the agonist site, the only accessible SH groups in purified AChR under the conditions used here should be the two cysteines at the agonist site. The EPR spectrum of rAChR modified with **II** is shown in Fig. 4A, and has features that are qualitatively similar to that seen for probe **I**. For probe **III**, Fig. 4B, both a motionally restricted and more mobile population can be observed; however, the probe is clearly much more isotropic in its motion when bound to AChR than either probes **I** or **II**. The averaged hyperfine coupling constants for probes **I**, **II** and **III** range from 16.5 to approximately 17 G, close to that usually obtained for nitroxide probes in an aqueous environment [28]. The reciprocal of the central linewidth resonance ΔH_0^{-1} and the reciprocal of the second moment of the EPR spectrum, $\langle H^2 \rangle^{-1}$, provide a measure of the amplitudes of motion for the nitroxide side chain on the ns time scale, and can be compared with the motion of nitroxides incorporated into specific protein sites [29]. From Figs. 1 and 4, the values

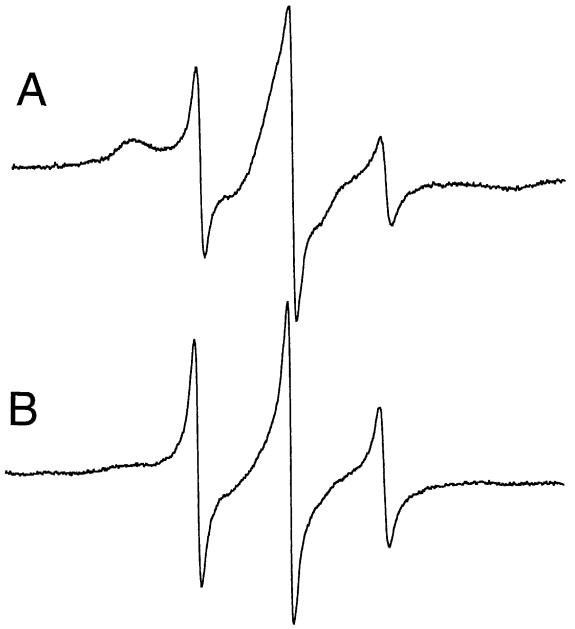

Fig. 4. EPR spectra of the maleimide probes **II** (A) and **III** (B) derivatized to reconstituted AChR following the procedure used in Fig. 1A.

of ΔH_0^{-1} were 0.33, 0.51 and 0.60 (G^{-1}) for probes **I**, **II** and **III**, respectively, while values of $\langle H^2 \rangle^{-1}$ were 3.68×10^{-3}, 3.70×10^{-3} and 4.90×10^{-3}, respectively. The values of $\langle H^2 \rangle^{-1}$ obtained for probes **I** and **II** are characteristic of nitroxide probes undergoing strong tertiary interactions with the protein structure, while the value for probe **III** is characteristic of a nitroxide that has relatively free rotation, such as that in a flexible loop. The values of ΔH_0^{-1} provide roughly the same information except that by this measure probe **II** appears to be similar to probe **III**. In spectra that are multicomponent, such as those shown here, the calculation of $\langle H^2 \rangle^{-1}$ emphasizes motional differences in the broader components, while ΔH_0^{-1} emphasizes differences in the more isotropic components [29]. These data indicate that these probes experience different levels of tertiary contact with the protein structure, with probe **I** showing the greatest level of contact followed in order by probes **II** and **III**.

3.3. Measurement of electrostatic potentials on membrane surfaces using power saturation

In order to determine whether power saturation EPR can be used to measure electrostatic potentials at

Table 1
Membrane surface potentials estimated using continuous wave power saturation on extruded unilamellar PC/PS containing membranes [a]

mol% PS	$\Delta P_{1/2}$ Tempo-OH (mW)	$\Delta P_{1/2}$ Tempo-NH_3 (mW)	Calculated ψ_s (mV)	Expected ψ_s (mV)
0	0.94	1.18	−5	0
7	1.10	2.65	−23	−17
15	0.81	3.24	−32	−32
25	0.95	4.31	−36	−43

[a] Based on the reproducibility of the EPR measurements and fitting of the $P_{1/2}$ values, we estimate the error in the calculated surface potentials to be approximately ±20% of the value of the potential, or ±5 mV, whichever is greater.

protein spin-labeled sites, measurements of the electrostatic surface potential on a membrane containing negatively charged lipid were made. These surface potentials have been extensively characterized using a number of techniques and are known to be accurately accounted for in the case of monovalent lipids by the Gouy–Chapman–Stern (GCS) model [14]. To measure the potential using power saturation, the uncharged ^{14}N alkyl-amide nitroxide label, **IV**, was incorporated into extruded vesicles on both membrane surfaces. Using a depth measurement described elsewhere [25], this nitroxide was found to lie between the 5-doxyl stearic acid spin-label and the headgroup, and is therefore well within the membrane interface. Power saturation measurements were then made in the presence and absence of the uncharged ^{15}N hydroxytempo, **V**, and the positively charged ^{15}N amino-tempo, **VI**, spin probe. These probes are membrane permeable and both internal and external populations of membrane bound spin-probe see the same concentration of water soluble probe. It should be noted that the ^{15}N probes contain a small amount of the ^{14}N isotope. The amplitude due to this component was corrected by subtraction, but usually made only a minor change in the estimated potential [2].

[2] One complication encountered in this experiment was the presence of a small level of ^{14}N spin-labeled nitroxide in the ^{15}N nitroxide samples. Because of the high concentrations of these probes, a 99% pure sample produces a measurable intensity in the central $m_I = 0$ resonance of the ^{14}N spin-label. In all cases examined here, this contribution was never greater than 15% of the ^{14}N label amplitude. The presence of the ^{14}N signal in the ^{15}N label could be corrected by subtracting the power saturation curve for the ^{14}N signal in the absence of the ^{14}N probe. This correction changed the estimate of the membrane surface potential by at most 5–10% in the cases examined here.

Shown in Table 1 are the $\Delta P_{1/2}$ values for probe **IV** produced by addition of 2 mM ^{15}N hydroxy-tempo and 2 mM ^{15}N amino-tempo. In the absence of any added PS, the two labels produce approximately the same change in the power saturation behavior of the membrane bound ^{14}N label within experimental error. This is expected because the two labels have the same size and the PC membrane surface is uncharged. As the membrane charge density is increased, the effect of the uncharged label **V** remains nearly the same, while the $\Delta P_{1/2}$ value for the positively charged probe **VI** increases. This increase in $\Delta P_{1/2}$ is a result of an enhanced collision frequency of the ^{15}N label with the membrane bound ^{14}N label, producing an enhancement in the T_{1e} of the bound nitroxide. Using Eq. (4) an experimental estimate of ψ_s was obtained and is also shown in Table 1. Comparison with the values of ψ_s predicted by the Gouy–Chapman–Stern model with the experimental estimate shows generally good agreement and indicates that this is a valid approach to estimate membrane surface potentials.

3.4. Estimate of the electrostatic potential near the agonist site

Using the procedure described above, electrostatic potentials on the AChR were measured at the positions of probes **I**, **II** and **III** from the values of $\Delta P_{1/2}$ obtained in the presence of **V** or **VI**. Table 2 shows the values for $\Delta P_{1/2}$ obtained in the presence of ^{15}N hydroxy-tempo and ^{15}N amino-tempo for rAChR in EPC labeled with **I** at an ionic strength of about 100 mM. From Eq. (4), the calculated potential is −15.8 mV. Also shown in Table 2 are the $\Delta P_{1/2}$ values for probes **II** and **III** covalently derivatized to the AChR in the presence of probes **V** or **VI**. These probes

Table 2
Potentials at the AChR agonist site estimated using continuous wave power saturation

Probe	$\Delta P_{1/2}$ Tempo-OH (mW)	$\Delta P_{1/2}$ Tempo-NH_3 (mW)	Estimated ψ_s (mV)
I (MBTA-SL)	8.1	15.22	−15.8
II	3.8	4.9	−5.9
III	4.0	4.0	0.0

[a] ^{15}N amino-tempo and ^{15}N hydroxy-tempo were used at a concentration of 1 mM.

produce a substantially lower estimate of the potential at the labeled site.

4. Discussion

The EPR spectra of the MBTA analog **I** shown in Fig. 1 indicates that the two agonist sites on the AChR are non-equivalent, and that the label when bound to the second site is less constrained and undergoing less contact with the protein structure than in site 1. The reasons for this difference are not clear, but must result from a larger volume available to the probe when derivatized to the second site. That these two sites are different is not surprising, the sites are believed to reside at two non-equivalent subunit interfaces [2,3], they show differences in their affinity towards toxins, and Cys^{192} and Cys^{193} are more difficult to reduce in site 2 [11]. When bound to the 'easily' labeled site, site 1, the spectrum is characteristic of a nitroxide that is undergoing strong tertiary contact with the protein structure. The spectrum clearly shows evidence for two components as do the maleimide labels **II** and **III**. These two components could be due to labeling at the two cysteine positions, two different conformations of the receptor, or different conformeric forms of the probe. There is precedence for this later possibility as sulfhydryl-specific nitroxide probes that can exist in several conformeric forms show similar types of spectra [29]. Previous work on the maleimide spin label **II** in native AChR containing membranes also showed evidence for multiple populations of label [30,31]; however, both the AChR and the peripheral 43-kDa protein were labeled and the heterogeneity in this case was attributed to non-specific labeling of reduced disulfides. In the present case, (see Section 3: Results) there is little non-specific labeling of the rAChR and this does not appear to be the appropriate explanation for the lineshapes shown here.

From the lineshapes, the nitroxide of the MBTA analog **I** appears to be in stronger contact with the receptor than either maleimide labels **II** or **III**. This is not unexpected as probe **I** should be a good analog for the agonist site. The spectrum of probe **III** is significantly more isotropic and shows less evidence for association with the protein than either probes **I** or **II**. This is an indication that this probe is extended from the agonist site. The linker in probe **III** would allow it to extend an additional 6–7 Å compared to the maleimide probe **II**.

In the present study, we used power saturation EPR spectroscopy to determine electrostatic potentials at negatively charged membrane surfaces and at the agonist site on the AChR reconstituted into vesicles. In lipid bilayers, the local concentration of ^{15}N labeled nitroxides can be effectively probed by examining the power saturation behavior of ^{14}N nitroxide labels, and the $\Delta P_{1/2}$ values used to estimate the membrane surface potential. Because the membrane surface potential has been so well characterized [14,32–34], it provides an excellent test for the approach and assumptions made here. For example, under the conditions used here ^{15}N labels are treated in a similar fashion to fast relaxing paramagnetic metals. The good agreement between the expected and measured potentials is a strong indication that for the conditions and potential range examined here these approximations are valid. It should be noted that this approach is not restricted to measurements of the membrane surface potential. In principle, this measurement could also be applied to the measurement of other membrane electric fields such as the dipole potential. In the case of the dipole potential,

measurements of the collisional frequency with charged species that cross the interface would permit an estimate of this potential.

The MBTA nitroxide analog **I** reported a potential of about -15 ± 3 mV at one of the agonist sites on the receptor, consistent with the proposed presence of negatively charged amino acid side chains at the agonist site [12]. This estimate is less than the value of -30 mV reported by measuring the kinetic salt effect of charged methanethiosulfonates [13]. That these measurements are different is not surprising as the nitroxide on probe **I** is not located at the same position as Cys^{192} or Cys^{193}; in addition, probe **I** also introduces an additional positive charge into the binding site. What is somewhat surprising is that the maleimide probe **II** reported less of a potential than probe **I**, and that probe **III** also reported no significant electrostatic potential. Probe **I** appears to interact most strongly with the agonist site followed by probes **II** and **III**, as indicated both by the values of ΔH_0^{-1} and the second moments of the spectra. Thus, the magnitudes of the electrostatic potentials appear to correlate with the interactions made by these labels. We speculate that the electrostatic potential at the agonist site exhibits significant spatial dependence, and that differences in these probes are a result of the different positions they occupy. At 100 mM ionic strength, the Debye length is approximately 10 Å. Given the size of these probes and possible distance from either Cys^{192} or Cys^{193}, this variation in electrostatic potential is not unreasonable.

It should be noted that the measurement of an electrostatic potential at these protein sites presumes that differences in the interactions of the soluble nitroxides **V** and **VI** with the protein bound nitroxides are entirely the result of electrostatics. Although these two probes are of virtually identical size, the measured potentials will not be accurate if there are significant differences in the steric interactions that these probes make with the binding site. The relaxation process measured here should be dominated by a contact or Heisenberg exchange, a process that takes place when nitroxides are separated by 4–5 Å. However, these probes clearly have some motion, and the potential that they sense will clearly be a spatial average of the conformations executed by the bound nitroxide label.

In conclusion, electrostatic potentials can be estimated at macromolecular surfaces by the use of continuous wave power saturation EPR. On membrane surfaces, these potentials are in agreement with other methods and with the predictions of the Gouy–Chapman–Stern theory. Using this approach, the electrostatic potential near the agonist site of the nicotinic acetylcholine receptor was estimated using a spin-labeled affinity probe **I** based on MBTA. The probe detected a small negative potential at this site, consistent with previous measurements and with the expected amino acid composition at the site. Two other sulfhydryl-specific probes were tested that show less contact with the protein and reported reduced electrostatic potentials. This likely reflects the spatial dependence of the potential at the agonist site.

Acknowledgements

This work was supported by grants from the National Science Foundation (IBN 9410788) and the National Institutes of Health (GM 35215).

References

[1] M. Noda, H. Takahashi, T. Tanabe, M. Toyosato, S. Kikyotani, Y. Furutani, T. Hirose, H. Takashima, S. Inayama, T. Miyata, S. Numa, Nature 301 (1983) 523–528.
[2] S.E. Pederson, J.B. Cohen, Biochemistry 87 (1990) 2785–2789.
[3] C. Czajkowski, A. Karlin, J. Biol. Chem. 266 (1991) 22603–22612.
[4] M. Dennis, J. Giraudat, F. Kotzyba-Hibert, M. Goeldner, C. Hirth, J.Y. Chang, C. Lazure, M. Chretien, J.P. Changeux, Biochemistry 27 (1988) 2346–2357.
[5] J.B. Cohen, S.D. Sharp, W.S. Liu, J. Biol. Chem. 266 (1991) 23354–23364.
[6] R.E. Middleton, J.B. Cohen, Biochemistry 30 (1991) 6987–6997.
[7] A. Karlin, M. Winnik, PNAS 60 (1968) 668–674.
[8] P.N. Kao, A. Karlin, J. Biol. Chem. 261 (1986) 8085–8088.
[9] P.N. Kao, A.J. Dwork, R.-R.J. Kaldany, M.L. Silver, J. Wideman, S. Stein, A. Karlin, J. Biol. Chem. 259 (1984) 11662–11665.
[10] R. Mosckovitz, J. Gershoni, J. Biol. Chem. 263 (1988) 1017–1022.
[11] J.W. Walker, C.A. Richardson, M.G. McNamee, Biochemistry 23 (1984) 2329–2338.
[12] C. Czajkowski, C. Kaufmann, A. Karlin, Proc. Natl. Acad. Sci. USA 90 (1993) 6285–6289.

[13] D.A. Stauffer, A. Karlin, Biochemistry 33 (1994) 6840–6849.
[14] S.A. McLaughlin, Annu. Rev. Biophys. Biophys. Chem. 18 (1989) 113–136.
[15] B. Honig, A. Nicholls, Science 268 (1995) 1144–1149.
[16] Y.-K. Shin, W.L. Hubbell, Biophys. J. 61 (1992) 1443–1453.
[17] D. Marsh, in: L.J. Berliner, J. Reuben (Eds.), Spin-Labeling, Theory and Applications, Vol. 8, Plenum, New York, 1989, pp. 255–303.
[18] J.S. Hyde, J.B. Feix, in: L.J. Berliner, J. Reuben, (Eds.), Spin-Labeling, Theory and Applications, Vol. 8, 1989, Plenum, New York, pp. 305–337.
[19] V.N. Damle, M. McLaughlin, A. Karlin, Biochem. Biophys. Res. Commun. 84 (1978) 845–851.
[20] G.R. Bartlett, J. Biol. Chem. 243 (1959) 466–468.
[21] E.L.M. Ochoa, A.W. Dalziel, M.G. McNamee, Biochim. Biophys. Acta 727 (1983) 151–162.
[22] C.R. Moore, J.R. Yates, P.R. Griffin, J. Shabanowitz, P.A. Martino, D.F. Hunt, D.S. Cafiso, Biochemistry 28 (1989) 9184–9191.
[23] P.K. Smith, R.I. Krohn, G.T. Hermanson, A.K. Mallia, F.h. Garter, M.D. Provenzano, E.K. Fujimoto, N.M. Goeke, B.J. Olson, D.C. Klenk, Anal. Biochem. 150 (1986) 76–85.
[24] U.K. Laemmli, Nature 227 (1970) 680–685.
[25] C. Altenbach, D.A. Greenhalgh, H.G. Khorana, W.L. Hubbell, Proc. Natl. Acad. Sci. USA 91 (1994) 1667–1671.
[26] W.L. Hubbell, C. Altenbach, in: S.H. White (Ed.), Membrane Protein Structure. Experimental Approaches, Oxford University Press, Oxford, 1994, pp. 224–248.
[27] C. Altenbach, T. Marti, G. Khorana, W. Hubbell, Science 248 (1990) 1088–1092.
[28] J.D. Morrisett, in: L. Berliner (Ed.), Spin Labeling, Theory and Applications, Academic Press, New York, 1976, pp. 273–338.
[29] H. Mchaourab, M. Lietzow, K. Hideg, W. Hubbell, Biochemistry 35 (1996) 7692–7704.
[30] A. Rousselet, J. Cartaud, P.F. Devaux, Biochim. Biophys. Acta 648 (1981) 169–185.
[31] V. Abadji, D.E. Raines, L.A. Dalton, K.W. Miller, Biochim. Biophys. Acta 1184 (1994) 25–34.
[32] J.D. Castle, W.L. Hubbell, Biochemistry 15 (1976) 4818–4831.
[33] S.A. McLaughlin, Curr. Topics Membr. Transp. 9 (1977) 71–144.
[34] D. Cafiso, A. McLaughlin, S. McLaughlin, A. Winiski, Methods Enzymol. 171 (1989) 342–364.